

Single Crystal Growth of Zirconium Nitride by Modified Filament-Method

Kohzo SUGIYAMA, Kunio WATANABE, Seiji MOTOJIMA,* and Yasutaka TAKAHASHI

Department of Synthetic Chemistry, Faculty of Engineering, Gifu University, Kakamigahara, Gifu 504

(Received June 2, 1978)

Single crystals of zirconium nitride (ZrN) have been grown by the modified filament-method from a gas mixture of ZrCl_4 , N_2 , H_2 , and Ar. The cubic crystals grew at 2000—2200 °C with a gas flow ratio $2\text{N}_2/\text{ZrCl}_4$ of 2—6, and evaporation of ZrN took place above 2400 °C. Linear growth rates along the $\langle 100 \rangle$ direction have been measured in terms of sequential micrographs, and attained a maximum of 60—75 $\mu\text{m}/\text{min}$ at 2100—2200 °C. The atomic ratio N/Zr of grown crystals increased with an increase of the flow ratio $2\text{N}_2/\text{ZrCl}_4$, and reached a constant of 0.93 above the flow ratio of 3.

Zirconium nitride, a representative interstitial compound of NaCl-type structure, has desirable properties such as high melting point (2982 °C;¹⁾ 3700 ± 70 °C at P_N , 60 atm²⁾), high hardness (≈ 2500 kg/mm²),³⁾ metallic conductivity and high resistivity at high temperature.

The preparation of single crystals of refractory compounds is difficult because of the high melting point. Crystal growth using a floating zone technique⁴⁾ is the only way by which single crystals have been successfully grown. Single crystals of the nitride,⁵⁾ diboride,⁶⁾ and carbide⁷⁾ of titanium have been grown by the authors using a modified filament-method, which has the advantages of simple procedure and apparatus. In this paper, the single crystal growth of zirconium nitride by the modified filament-method will be described.

Experimental

Apparatus and Growth Procedure. The apparatus is analogous to that used in previous experiments on titanium nitride crystal growth.⁵⁾ A tungsten filament (99.0% pure) 30 mm long and 0.3 mm thick was tightly bound to iron electrodes 5.8 mm thick. Another short tungsten wire of 0.3 mm diameter was twisted around the tungsten filament (one and a half turns) and the tips cut slantwise with a separation of 0.3—1.0 mm from the filament and pointing towards the gas inlet. The filament was located in a horizontal reaction tube (24 mm in i.d.) which was heated to 400 °C by a nichrome heater thereby keeping zirconium tetrachloride in the vapor phase. Zirconium tetrachloride was prepared by the chlorination of zirconium sponge (99.9% pure) at 550 °C, and carried into the reaction zone by argon gas. The flow rate of zirconium tetrachloride was calculated assuming quantitative chlorination to the tetrachloride. Hydrogen and nitrogen were mixed with the zirconium tetrachloride stream near the filament. The surface temperature of the growing crystals was measured by an optical pyrometer through an observation window.

Measurement of Linear Growth Rate. The growing crystals were photographed using a stereoscopic microscope every 10—20 s. A series of sequential micrographs is shown in Fig. 1. The linear growth rate along the $\langle 100 \rangle$ direction was obtained as the gradient from the plot of edge length versus growth time.

Atomic Ratio (N/Zr) in Crystals and the Lattice Constant. A collection of zirconium nitride crystallites was pulverized, and oxidized to zirconium dioxide at 1000 °C for 5 h in an oxygen flow. The atomic ratio N/Zr was calculated from the weight of zirconium nitride crystallites W_{ZrN} and zirconium dioxide W_{ZrO_2} , using the following equation;

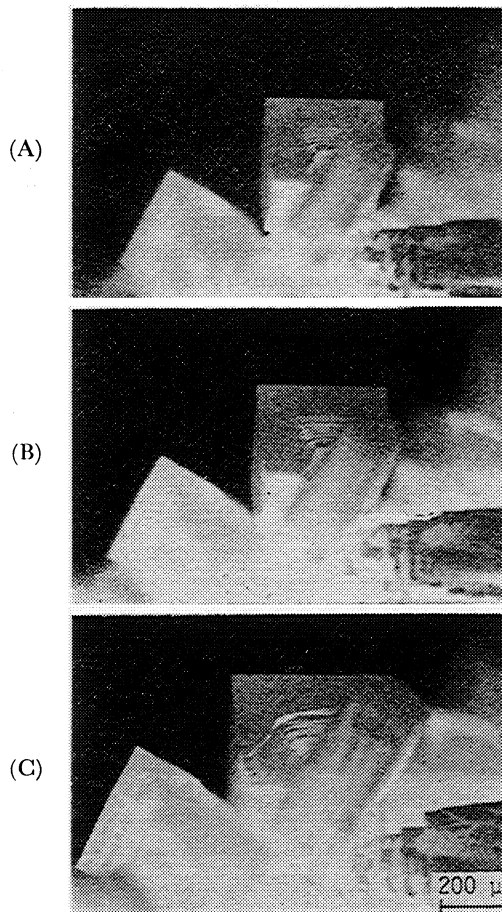


Fig. 1. Sequential micrographs of the growing crystals. Temperature: 2000 °C, $2\text{N}_2/\text{ZrCl}_4$: 5.4, $2\text{H}_2/\text{ZrCl}_4$: 10, total flow rate: 3.0 cm³/s, growth time: (A) 0 min (starting of measurement), (B) 4 min, (C) 15 min.

$$\text{N/Zr} = 8.7972(W_{\text{ZrN}}/W_{\text{ZrO}_2}) - 0.7403. \quad (2)$$

The lattice constant was determined by X-ray diffraction using annealed silicon powder as internal standard.

Micro-hardness. Micro-hardness was measured by a Vickers micro-hardness tester (Akashi, MVK-C) on the (100) and (111) facets of cubic and tetragonal pyramid crystals, respectively.

Results and Discussion

Crystal Morphology. The effect of growth temperature and source gas flow ratio $2\text{N}_2/\text{ZrCl}_4$ ("N/Zr ratio" hereafter) on crystal morphology is shown in Fig. 2, in which the sum of the flow rates of zirconium tetra-

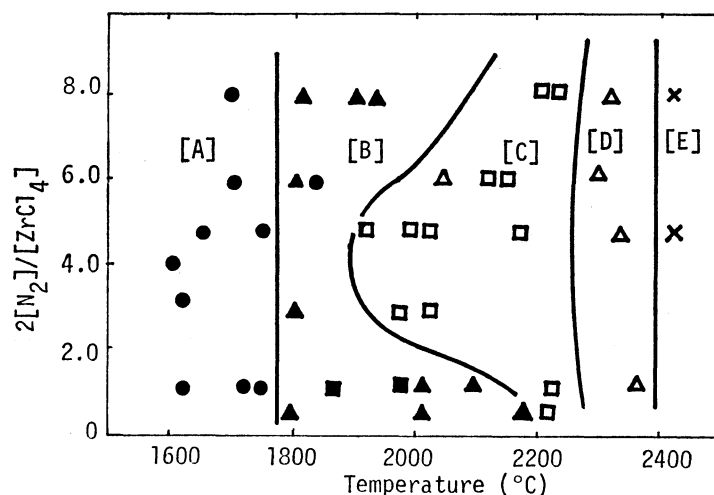


Fig. 2. Effect of the temperature and the flow ratio ($2N_2/ZrCl_4$) on crystal morphology. Total flow rate: $3.0 \text{ cm}^3/\text{s}$, $ZrCl_4 + N_2$: $0.1 \text{ cm}^3/\text{s}$, $2H_2/ZrCl_4$: 3.

(●) Coatings or fine crystals, (▲) tetragonal pyramid crystals, (■) polyhedral crystals, (□) cubic crystals, (△) arrow-like or dendritic crystals, (×) no-deposition.

[A] Coating or fine crystal growth region, [B] tetragonal pyramid crystal growth region, [C] cubic crystal growth region, [D] arrow-like or dendritic crystal growth region, [E] no deposition region.

chloride and nitrogen was kept at $0.1 \text{ cm}^3/\text{s}$ and the gas flow ratio $2H_2/ZrCl_4$ ("H/Zr ratio" hereafter) kept at 3. The crystal morphology varied with increase in growth temperature in the following order; polycrystallite or fine crystal, tetragonal pyramid, cubic, and arrow-like or dendritic. Cubic crystals grew in the temperature range of 2000 – 2200°C and at a N/Zr ratio of 2–6. Above 2400°C , the crystals did not grow and crystallites which had been deposited at a lower temperature gradually disappeared. Concerning the evaporation of zirconium nitride, Hoch *et al.*⁸⁾ have investigated the evaporation in the temperature range of 2236 – 2466 K . Extrapolating the data of Hoch *et al.*

to 2400°C , the evaporation rate is given by the curve B in Fig. 8, and is as fast as $85 \mu\text{m}/\text{min}$ at 2400°C . This evaporation temperature is 200°C higher than that of titanium nitride.⁵⁾

The effect of growth temperature and H/Zr ratio on crystal morphology is shown in Fig. 3, in which the N/Zr ratio was kept constant at 4. The growth regions of the pyramidal and arrow-like or dendritic crystals spread to the hydrogen-rich region (Fig. 3, regions B and D). Cubic crystals grew in the temperature range of 2100 – 2300°C under a H/Zr ratio below 40.

In Figs. 4 and 5, the representative morphologies of zirconium nitride crystals are shown. Large cubic or

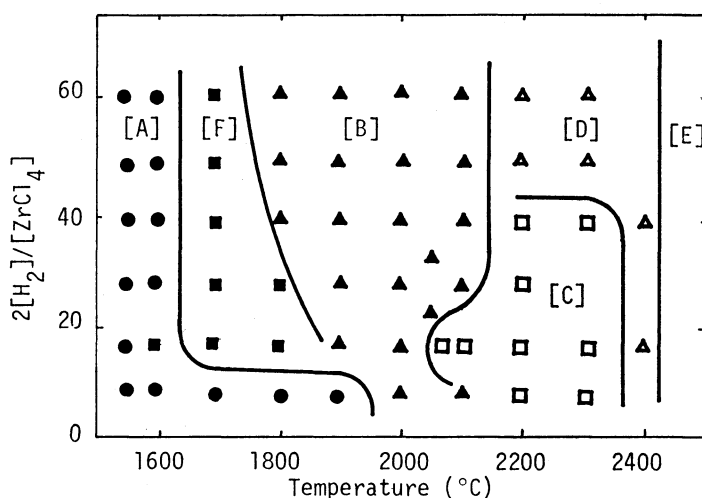


Fig. 3. Effect of the temperature and the flow ratio ($2H_2/ZrCl_4$) on crystal morphology. Total flow rate: $3.0 \text{ cm}^3/\text{s}$, $2N_2/ZrCl_4$: 4. [F] polyhedral crystal growth region. Signs and other notations are the same as those of Fig. 2.

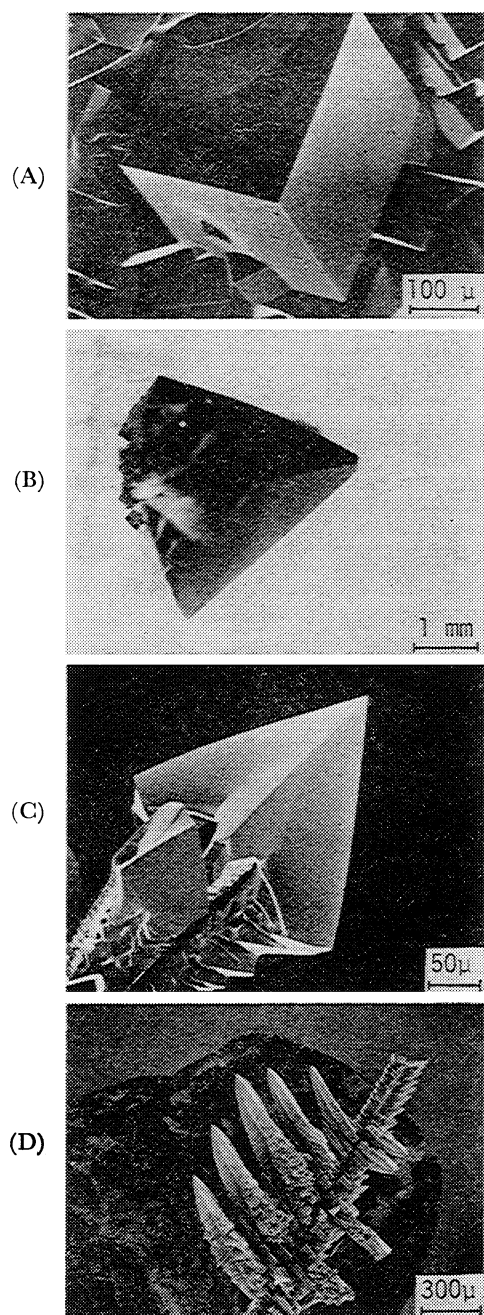


Fig. 4. Representative morphologies of zirconium nitride crystals. (A) cubic crystal, temperature: 2000 °C; $2\text{N}_2/\text{ZrCl}_4: 4$, (B) tetragonal pyramid crystals, (C) tetragonal pyramid crystal, temperature: 1800 °C; $2\text{H}_2/\text{ZrCl}_4: 4$, (D) arrow-like and dendritic crystals, temperature: 2300 °C; $2\text{N}_2/\text{ZrCl}_4: 4$.

tetragonal pyramidal crystals grew from the tips of the tungsten wire, after initial deposition of a few nuclei (Fig. 5). The largest single crystals obtained in this work were 3 mm in edge length for cubic crystals and 3.5 mm for tetragonal pyramids for 90 min growth under a condition of C- and B-regions in Fig. 2, respectively. Square pillar crystals of 10 μm thickness and 1 mm length, on which short pillar crystals branched perpendicularly, were obtained by chance on the filament close to the bound point of the electrodes (Fig. 6). X-Ray diffraction profiles of the pillar crystals are



Fig. 5. Cubic crystal grown on the tip of tungsten wire.

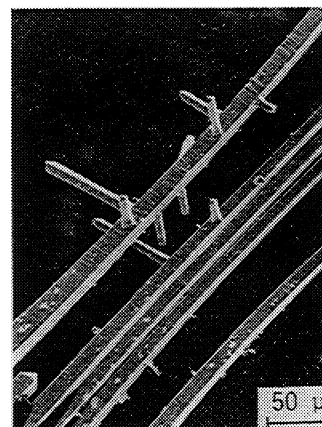


Fig. 6. Square pillar crystals.

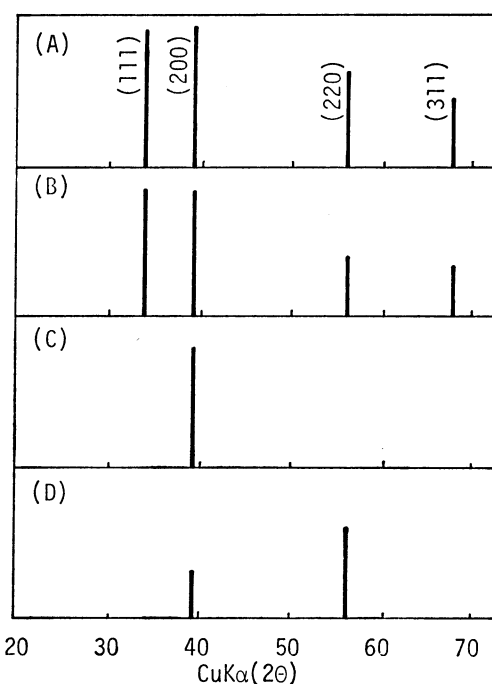


Fig. 7. X-Ray diffraction profiles (A) ZrN-ASTM (No. 2-956), (B) pulverized from crystallites, (C) a square facet of cubic crystal, (D) square pillar crystals set aside along the growth axis.

shown in Fig. 7D, together with those of pulverized crystallites (Fig. 7B) and the square facet of a cubic crystal (Fig. 7C). The pillar crystal was suspended in a

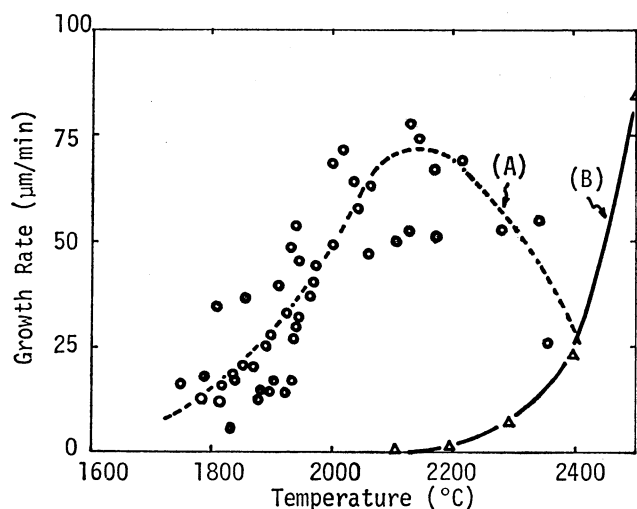


Fig. 8. (A) Effect of the temperature on the linear growth rate in $\langle 100 \rangle$ direction. Total flow rate: $3.0 \text{ cm}^3/\text{s}$, $2\text{N}_2/\text{ZrCl}_4$: 4, $2\text{H}_2/\text{ZrCl}_4$: 15. (B) Evaporation rate.⁹⁾

drop of water, poured on to a holder plate and dried. Thus, the growth axis of the pillar crystals may be regarded as parallel to the holder plate. The two strong peaks in Fig. 7D have been assigned as (200) and (220) of the cubic lattice and thus, the growth direction is considered to be $\langle 100 \rangle$.

Linear Growth Rate. *Dependence on Temperature:* The linear growth rate along the $\langle 100 \rangle$ direction of a cubic crystal was measured in the temperature range of 1700–2400 °C as shown in Fig. 8, in which the N/Zr and H/Zr ratios were kept constant at 4 and 15, respectively. The growth region for tetragonal pyramid crystals is below 1900 °C and for arrow-like crystals above 2250 °C, as seen in Fig. 2. The linear growth rate along the $\langle 100 \rangle$ direction in the temperature range was measured as follows; a few small cubic crystals were deposited on the tip in the temperature range C in Fig. 2, followed by decreasing or increasing the temperature to that of measurement. The growth rate increased with the increase of temperature and reached a maximum (about $75 \mu\text{m}/\text{min}$) in the temperature range 2100–2200 °C, and decreased above 2200 °C. Dispersion of the data may be attributed to fluctuation of the nucleation site, the size and the orientation of the crystals, and the temperature of the growing crystals.

Dependence on N/Zr Ratio: The effect of the N/Zr ratio on the linear growth rate along the $\langle 100 \rangle$ direction was examined, where the sum of the flow rates of zirconium tetrachloride and nitrogen, and the H/Zr ratio were kept constant at $0.1 \text{ cm}^3/\text{s}$ and 10, respectively. The maximum growth rates of 60 and $35 \mu\text{m}/\text{min}$ were measured under a N/Zr ratio of 2–3 at 2100 °C and 1.5–2.5 at 1900 °C, respectively. These values are in agreement with that of the polycrystalline growth of zirconium nitride from the same gas mixture at 1150 °C.⁹⁾

Dependence on H/Zr Ratio: The effect of the H/Zr ratio on the linear growth rate was examined, where the N/Zr ratio was kept constant at 4. The linear growth rate increased with increase of the H/Zr ratio and the

maximum was at a ratio as high as 15–18 at 2100 °C, the rate decreasing abruptly above these ratios. At a H/Zr ratio above 40, that is, a low flow ratio of zirconium tetrachloride, the growth rate along the $\langle 111 \rangle$ direction predominated resulting in arrow-like or dendritic growth.

Dependence on the Total Flow Rate: The effect of the total flow rate on the growth rate along the $\langle 100 \rangle$ directions was examined, where N/Zr and H/Zr ratios were kept constant at 4 and 10, respectively, and the temperature at 2000 °C. The growth rate increased with increase of the total flow rate approaching a constant value of $45 \mu\text{m}/\text{min}$ above a flow rate of $3 \text{ cm}^3/\text{s}$ which corresponds to a linear velocity at the growth temperature of about $5 \text{ cm}/\text{s}$.

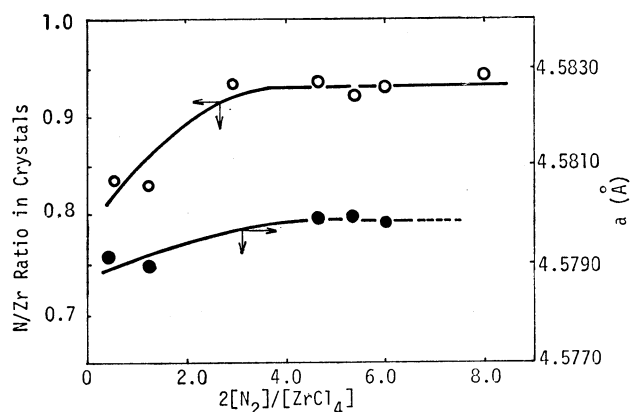


Fig. 9. Effect of flow ratio ($2\text{N}_2/\text{ZrCl}_4$) on the atomic ratio (N/Zr) and the lattice constant in ZrN crystals. Temperature: 2000–2100 °C, total flow rate: $3.0 \text{ cm}^3/\text{s}$, $2\text{H}_2/\text{ZrCl}_4$: 15.

The Atomic Ratio N/Zr in Crystals and Lattice Constant.

The influence of the N/Zr ratio in input gas on the atomic ratio N/Zr in crystals and the lattice constant are shown in Fig. 9, in which the crystals were grown in the temperature range of 2000–2100 °C and with a H/Zr ratio of 15. The atomic ratio N/Zr in crystals increased with the increase of N/Zr ratio in input gas attaining a constant value of 0.93 at a flow ratio above 3. Zirconium nitride exists over a broad composition range corresponding to $\text{ZrN}_{0.55-1.0}$ ¹⁰⁾ and $\text{ZrN}_{1.54-1.0}$ at 1500 °C.¹¹⁾ The stoichiometric composition of ZrN could not be obtained in the present work and the lowest atomic ratio N/Zr was about 0.83.

The lattice constants of zirconium nitride crystals were 4.579 Å for a sample of N/Zr=0.83 and 4.580 Å for that of 0.93. These values are slightly larger than those reported in the literature; i.e. 4.5755 Å (N/Zr=0.89),¹²⁾ 4.564 Å (N/Zr=1.0),¹³⁾ and 4.5755 Å (N/Zr=0.93).¹⁴⁾ The deviations of the constants from the literature may arise from the presence of oxygen in the crystal lattice,¹⁵⁾ although the presence of oxygen in the crystal was below the detectable limit of electron probe microanalysis.

Micro-hardness. Micro-hardness was measured on the (100) and (111) facets of cubic and tetragonal pyramid crystals, respectively. The hardness varied from 1500 to $1600 \text{ kg}/\text{mm}^2$, irrespective of the crystal

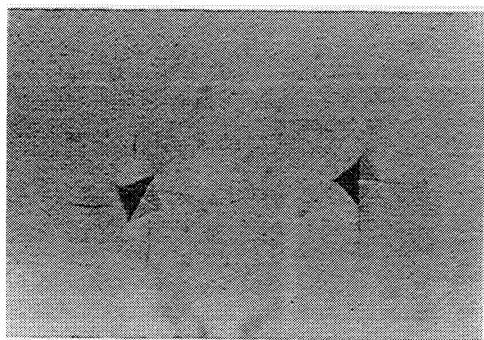


Fig. 10. Typical marks impressed on the (100) facet of a cubic crystal by a pyramidal diamond indenter in Vickers microhardness tester.

facets. These values are somewhat smaller than that reported by Hill *et al.*³⁾ Typical marks impressed on the (100) facet of cubic crystals by a pyramidal diamond indenter are shown in Fig. 10. Slip lines can be seen in the $\langle 110 \rangle$ direction irrespective of the orientation of the indenter, which is in agreement with the slip direction of titanium nitride.¹⁶⁾

References

- 1) L. E. Toth, "Transition Metal Carbides and Nitrides," in "Refractory Materials," ed by J. L. Margrave, Academic Press, New York and London (1971), Vol. 7.
- 2) M. A. Eron'yan, R. G. Avarbe, and T. A. Nikol'skaya, *Zh. Prikl. Khim. (Leningrad)*, **46**, 428 (1973); *Chem. Abstr.* **78**, 140540 m (1973).
- 3) R. J. Hill, S. Scheuermann, and R. Lucariello, *Thin Solid Films*, **40**, 217 (1977).
- 4) A. N. Christensen, *J. Cryst. Growth*, **33**, 99 (1976).
- 5) S. Motojima, K. Baba, K. Kitatani, Y. Takahashi, and K. Sugiyama, *J. Cryst. Growth*, **32**, 141 (1976).
- 6) K. Sugiyama, S. Iwakoshi, S. Motojima, and Y. Takahashi, *J. Cryst. Growth*, **43**, 533 (1978).
- 7) K. Sugiyama, H. Mizuno, S. Motojima, and Y. Takahashi, unpublished data.
- 8) M. Hoch, D. P. Dingley, and H. L. Johnston, *J. Am. Chem. Soc.*, **77**, 304 (1955).
- 9) T. Takahashi, H. Itoh, and S. Noguchi, *Nippon Kagaku Kaishi*, **1975**, 627.
- 10) E. K. Stromes, *M. T. P. Int. Rev. Sci., Inorg. Chem. Ser. I*, **37** (1972).
- 11) E. D. Rudy and F. Benesovsky, *Monatsh. Chem.*, **92**, 415 (1961).
- 12) C. R. Houska, *J. Phys. Chem. Solids*, **25**, 359 (1964).
- 13) G. V. Samsonov and T. S. Verkhoglyanova, *Dopov. Akad. Nauk Ukr. RSR*, **1962**, 48.
- 14) J. G. Desmaison and W. W. Smeltzer, *J. Electrochem. Soc.*, **122**, 354 (1975).
- 15) N. Schönberg, *Acta Chem. Scand.*, **8**, 627 (1954).
- 16) F. W. Vahldiek and S. A. Mersol, *J. Less-Common Met.*, **55**, 265 (1977).